

**DIASTEREOISOMERIC PROTON-BOUND COMPLEXES OF
1,5-DIAZA-*cis*-DECALIN IN THE GAS PHASE**Jana ROITHOVÁ^{a,b}^a Department of Organic Chemistry, Faculty of Science, Charles University,
Hlavova 8, 128 40 Prague 2, Czech Republic; e-mail: roithova@natur.cuni.cz^b Institute of Organic Chemistry and Biochemistry, Academy of Sciences of the Czech Republic, v.v.i.,
Flemingovo nám. 2, 166 10 Prague 6, Czech Republic; e-mail: roithova@uochb.cas.cz

Received September 11, 2008

Accepted November 10, 2008

Published online February 14, 2009

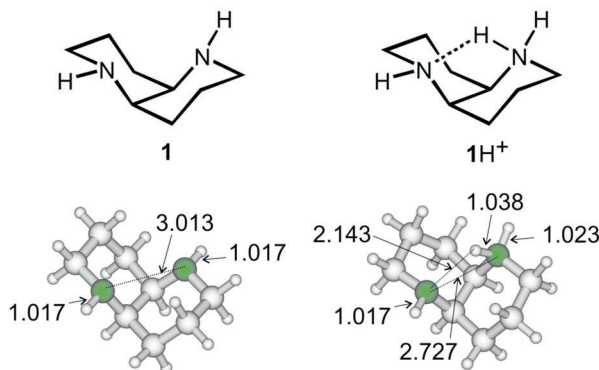
Diastereoisomeric proton-bound complexes of 1,5-diaza-*cis*-decalin (**1**) with butan-2-amine (**2**) are studied by means of the DFT calculations and mass spectrometry. The calculations reveal that **2** is bound via proton to only one nitrogen atom of the bicyclic base **1**. The homochiral complex is favored by about 4 kJ/mol over the heterochiral complex. For a more loosely bound ion-pair complex [(1H)I(2H)]⁺ of the protonated bases **1** and **2** with an iodine counterion the energy difference drops to about 2 kJ/mol. Chiral effects in the formation of [(1)H(2)]⁺ are studied by the collision-induced dissociation of [(1H)I(2H)]⁺ generated by the electrospray ionization of the solution of [1-Cu(OH)I] and **2** in acetonitrile. The dominant fragmentation of [(1H)I(2H)]⁺ leads to 1·H⁺ and 2·HI, which is at small collision energies accompanied by the elimination of HI leading to the desired [(1)H(2)]⁺ ion. The chiral effect of 1.2 is determined in favor for the formation of the homochiral complex [(1)H(2)]⁺.

Keywords: Basicity; Proton affinity; Chiral reactions; Diazadecalin; DFT calculations; Mass spectrometry; Gas phase complexes.

Chiral ligands have a unique role in the enantioselective synthesis of chiral compounds. A vast number of synthetic approaches nowadays use transition metals as catalytic centers for the mediation of chemical reactions. The stereoselective induction is usually achieved by a simple coordination of a chiral ligand to the catalytically active metal center. The bicyclic compound 1,5-diaza-*cis*-decalin (**1**) belongs to the ligands often used for reactions catalyzed by copper. For example, a complex of 1,5-diaza-*cis*-decalin with Cu(OH)I has been specially developed for the enantioselective synthesis of BINOL¹. The skeleton of 1,5-diaza-*cis*-decalin forms an unsymmetrical cavity with two nitrogen atoms at the apexes and both nitrogen atoms can be coordinated to a metal. The molecule of 1,5-diaza-*cis*-decalin represents therefore a bidentate ligand. Scheme 1 shows the most stable con-

former of **1** with proximal nitrogen atoms; the alternative arrangement, where the nitrogen atoms are in the distal positions becomes stable only if hydrogen atoms bound to nitrogen atoms are substituted by e.g. alkyl groups². Due to the fact that two nitrogen atoms are in spatial vicinity, compound **1** is also a strong base³. It has been theoretically predicted that its proton affinity amounts to 1033 kJ/mol (ref.³) and **1** can be therefore termed as a superbases. Although the two nitrogen atoms do not equally participate in the binding to a proton, the geometry changes associated with the protonation of **1** suggest that the non-protonated nitrogen atom also contributes to stabilization of the charge in the molecule (Scheme 1).

Here, a chiral discrimination in binding of protonated 1,5-diaza-*cis*-decalin with another chiral nitrogen base butan-2-amine (**2**) is investigated.



SCHEME 1

1,5-Diaza-*cis*-decalin (**1**) and the protonated molecule **1H⁺**. The selected bond lengths are in Å; carbon is in grey and nitrogen in green

EXPERIMENTAL

The experiments were performed with a TSQ Classic mass spectrometer which has been described elsewhere^{4,5}. Briefly, the TSQ Classic consists of an electrospray ionization (ESI) source combined with a tandem mass spectrometer of QOQ configuration (Q stands for quadrupole and O for octopole). The investigated ions were generated by ESI of solutions of [1-Cu(OH)I] and **2** in acetonitrile. All chiral compounds were purchased enantiomerically pure. The first quadrupole was used as a mass filter to scan the ion spectrum or to select a certain ion of interest; the mass resolution of the quadrupole was sufficient to fully resolve the isotope envelopes of the studied ions according to their m/z ratio. The mass-selected ions were then guided through the octopole serving as collision chamber followed by mass analysis of the collision-induced dissociation (CID) products by means of the second quadrupole and subsequent detection. Xenon was used as a collision gas and it was leaked into the octopole at pressure of 1×10^{-4} mbar, which corresponded to single-collision condi-

tions. The collision energy was adjusted by a relative potential between the first quadrupole and the octopole in the energy range $E_{\text{lab}} = 0\text{--}18$ eV. The kinetic energy resolution was determined by the retarding-potential analysis of the parent ions and the beam width at half maximum amounts to 2.0 ± 0.1 eV in the laboratory frame.

The calculations were performed at the B3LYP/6-31G**⁶⁻⁸ level of theory as implemented in the Gaussian 03 suite⁹. The structures are fully optimized and the minima verified by the analyses of the Hessian matrixes. The iodide-bound complexes are calculated using the B3LYP/SDD approach, where the basis set corresponds to the valence double ζ D95V¹⁰ and the core electrons of the iodine atom are described by Stuttgart/Dresden pseudopotentials¹¹. The energy values discussed below refer to enthalpies at 0 K and Gibbs energies at 298 K. The DFT method does not correctly describe the dispersion interaction in the studied systems, which can be sometimes important for the correct evaluation of chiral effects¹². However, it can be expected that in the positively charged saturated systems studied here, the dispersion interaction plays a minor role.

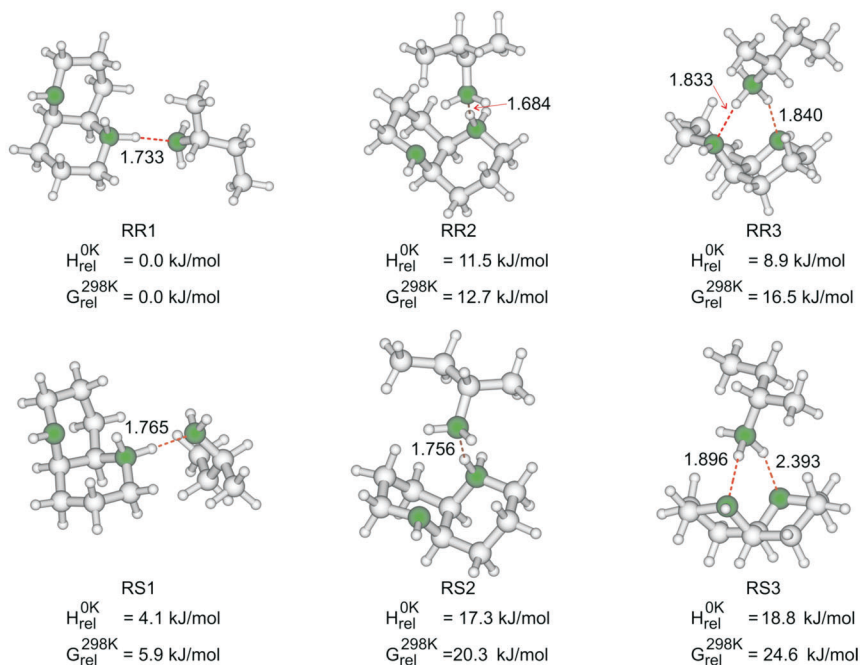
RESULTS AND DISCUSSION

First, the possible arrangements of the proton-bound complexes between 1,5-diaza-*cis*-decalin and butan-2-amine are investigated computationally. According to the B3LYP/6-31G** calculation the proton affinity of **1** amounts to 10.51 eV (1014 kJ/mol). The same methods provides the proton affinity of **2** as 9.82 eV (948 kJ/mol), which is in reasonable agreement with the experimental value of 9.64 eV¹³. Several optimized geometries of the proton-bound complexes are depicted in Scheme 2. The most stable arrangement of the homochiral and also heterochiral complexes (for the case of simplicity denoted as [(*R*-**1**)H(*R*-**2**)]⁺ and [(*R*-**1**)H(*S*-**2**)]⁺, respectively) corresponds to the situation, where the proton is bound to the stronger base **1** and **2** is bound to the outer hydrogen atom of the protonated nitrogen of **1** (isomers denoted as RR1 and RS1, respectively). In the less stable arrangements RR2 and RS2, **2** binds to the inner hydrogen atom of the protonated nitrogen of **1**, which on one hand leads to a shorter distance between **2** and the bridging proton and, consequently, the hydrogen bond might be stronger. However, on the other hand, there is a larger steric interaction between backbones of both the nitrogen bases, which results in overall larger potential energy of this arrangement. Finally, it is considered that proton might be bound to the weaker base **2** and the complex could be stabilized by a double hydrogen bonding to both nitrogen atoms of **1**. Such arrangements lead to stable structures RR3 and RS3 (see Scheme 2).

Obviously, in the most stable arrangements RR1 and RS1, the backbone interactions of the two bases are minimized, which results in a relatively small energy difference of 4 kJ/mol between the two diastereoisomers. On the other hand, in the remaining isomers, where the cavity of **1** is involved,

the energy differences are larger. The largest effect is found for the double hydrogen-bound diastereoisomers RR3 and RS3, where the energy discrimination between homochiral and heterochiral complexes reaches 10 kJ/mol. The formation of all complexes is an exothermic process. The formation of the complex RR1 is associated with an energy release of 86.6 kJ/mol at 0 K. If the Gibbs energies are considered, the exoergicity drops to 43.8 kJ/mol at 298 K. For the heterochiral variant RS1, the binding energy at 0 K amounts to 82.5 kJ/mol and the consideration of Gibbs energies at 298 K leads to a value of 37.9 kJ/mol.

The discrimination between formation of homochiral and heterochiral complexes can be investigated also experimentally in the gas phase by means of mass spectrometry^{14–22}. There are several possible approaches to probe the stability of different diastereoisomeric complexes in the gas phase. The easiest way consists in the investigation of the abundances of



SCHEME 2

Proton-bound complexes between 1,5-diaza-*cis*-decalin (**1**) and butan-2-amine (**2**). The complexes are denoted by two letters, the first one corresponds to the configuration of **1** and the second to the configuration of **2**. The selected bond lengths are in Å; carbon is in grey and nitrogen in green

the diastereoisomeric ions formed in the ion source. Such strategy usually requires labeling of one chiral variant of the studied compounds²³. Another strategy comes from the investigation of the fragmentation kinetics of various diastereoisomeric proton- or metal-bound complexes^{19,24,25} and also ion-molecule reactions can be used to differentiate diastereoisomeric complexes^{26,27}.

The electrospray ionization of the solution of $[1\cdot\text{Cu}(\text{OH})\text{I}]$ and **2** in acetonitrile leads surprisingly mainly to the formation of the protonated molecules and proton-bound complexes (Fig. 1). Complexes of copper are almost absent in the spectra, which might be due to a low solubility of the copper complex and also due to the fact that copper undergoes reduction under the conditions of ESI from the acetonitrile solution²⁸. A comparison of the peaks containing either **1** or **2** in the spectrum reveals that **2** forms easier proton-bound complexes as the abundance of $[\mathbf{2H}\cdot\text{CH}_3\text{CN}]^+$ and $[(\mathbf{2H})_2\text{I}]^+$ largely prevails the abundance of $\mathbf{2H}^+$. On the other hand, the sterically more demanding base **1** is mostly present as the naked protonated ion $\mathbf{1H}^+$ and the proton-bound complexes are less abundant. Interestingly, also a mixed complex $[(\mathbf{1H})\text{I}(\mathbf{2H})]^+$ is present in the spectrum, which most probably corresponds to an ion-pair complex of protonated bases **1** and **2** bound via the iodine anion. The source spectra are analogous for all combinations of enantiomers of **1** and **2** and therefore only the variant of the

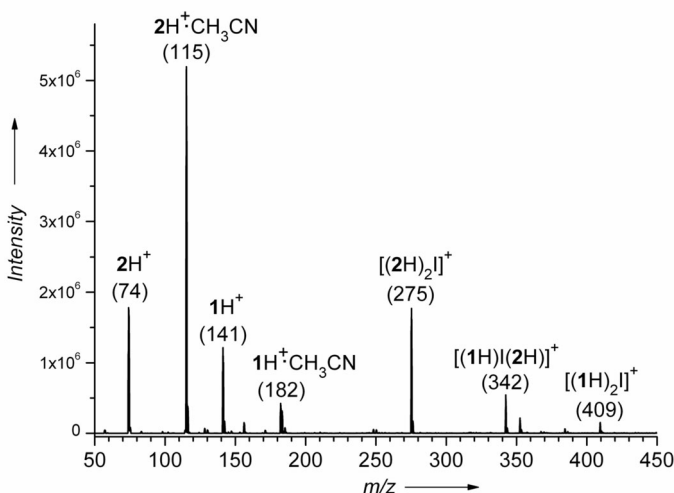


FIG. 1

The ESI source spectrum of a dilute solution of the complex between $[1\cdot\text{Cu}(\text{OH})\text{I}]$ and (*R*)-butan-2-amine (**2**) in acetonitrile

mixture of (*R*)-1,5-diaza-*cis*-decalin and (*R*)-butan-2-amine (in the following denoted as *R*-1 and *R*-2, respectively) is shown.

Collision-induced dissociation of the mixed complex $[(1H)I(2H)]^+$ leads predominantly to the elimination of neutral $[2\cdot HI]$ and formation of $[1H]^+$ (Fig. 2). The complementary fragmentation to $[1\cdot HI]$ and $[2H]^+$ can be observed at a larger collision energy (Fig. 2b). A larger collision energy can also induce subsequent fragmentation of $[1H]^+$ or $[2H]^+$ by loss of ammonia as revealed by peaks at m/z 124 and 57, respectively. At a small collision energy, another abundant fragmentation is detected, which corresponds to the loss of neutral HI from the complex $[(1H)I(2H)]^+$ and thus the formation of proton-bound complex $[(1)H(2)]^+$. The fragmentation of the diastereoisomers $[(1H)I(2H)]^+$ is investigated further in order to reveal possible preferences in the formation of homochiral or heterochiral diastereoisomer of $[(1)H(2)]^+$.

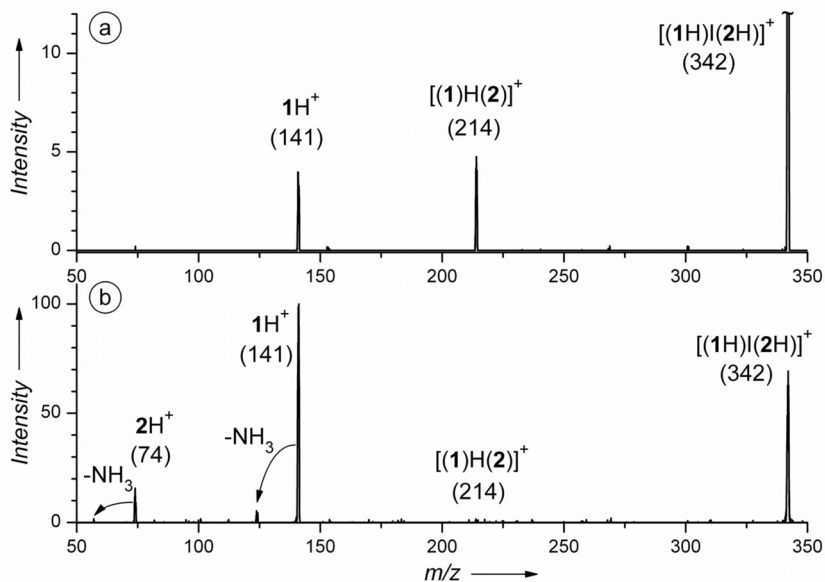
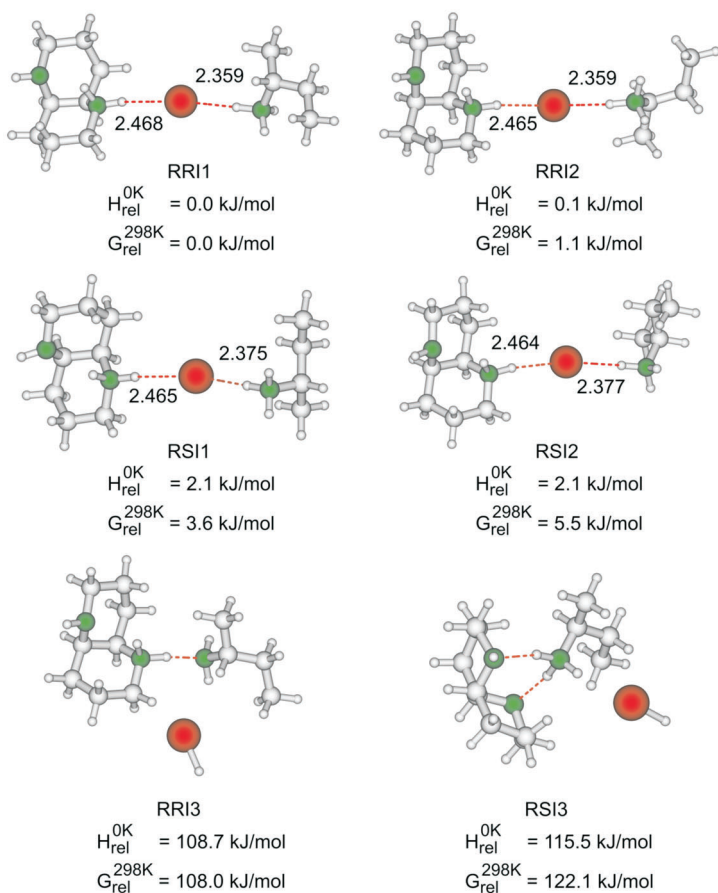


FIG. 2

The collision-induced dissociation spectra at the collision energy $E_{\text{coll}} = 0.3$ (a) and 5 eV (b) of the complex $[(2H)I(1H)]^+$ generated by ESI of a solution of $[1\cdot Cu(OH)I]$ and **2** in acetonitrile. The highest peaks in the spectra are normalized to 100; note that the parent ion is off-scale in Fig. 2a

As expected, the exploratory search on the potential-energy surface of $[(1\text{H})\text{I}(2\text{H})]^+$ suggests that the energy difference between the diastereoisomers of the iodide-bound complex of the protonated bases **1** and **2** is smaller than it was found for $[(1)\text{H}(2)]^+$. Scheme 3 shows several structures localized for the iodide bound complexes of the protonated bases. As the distance between the two protonated bases amounts to about 5 Å, the mutual interaction is only small. Several possible orientations of the two

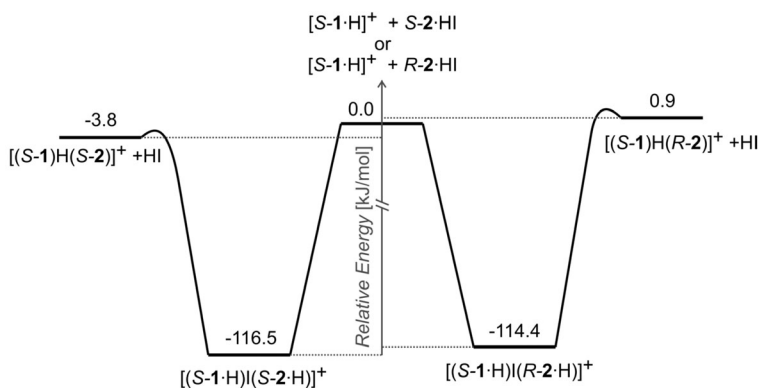


SCHEME 3

Proton-bound complexes between 1,5-diaza-*cis*-decalin (**1**) and butan-2-amine (**2**). The complexes are denoted by three letters, the first one corresponds to the configuration of **1**, the second to the configuration of **2** and the third stands for the iodide present. The selected bond lengths are in Å; carbon is in grey, nitrogen in green, and iodine in red

protonated bases can be found by a rotation of a base around the iodine–hydrogen bond. The rotation does not largely influence the distance between the two subunits and also the relative energies of the “rotamers” are not changed significantly as demonstrated by pairs of structures shown for the combination of *R*-1/*R*-2 (RRI1 and RRI2) and *R*-1/*S*-2 (RSI1, RSI2), respectively. The structural alternatives, where the molecule of HI is coordinated to the proton-bound complex of the bases **1** and **2**, lie significantly higher in energy (see selected isomers RRI3 and RSI3), therefore, it is expected that such isomers are not present in the ion beam.

Thus, it can be expected that the abundance of the HI elimination from the $[(1H)I(2H)]^+$ complexes can differ for different diastereoisomers of the complexes. According to the calculations, the elimination of HI from the homochiral complex is slightly less endothermic (by about 2 kJ/mol) and a similar effect can be expected for the corresponding energy barriers (Scheme 4). On the other hand, cleavage of the $[(1H)I(2H)]^+$ complex to the chiral subunits $1 \cdot H^+$ and $2 \cdot HI$ is less energy demanding for the heterochiral complexes. Thus, both effects should in synergy favor the HI elimination for the homochiral complex. It is noted in passing that the transition structures for the HI elimination were not calculated due to the size of the studied system.



SCHEME 4

Schematic drawing of the potential-energy surface for the dissociation of homochiral and heterochiral complex $[(1H)I(2H)]^+$. Energies are obtained from the B3LYP/SDD calculations and are considered at 0 K. Note that the use of a different basis set leads to a slightly larger energy difference between proton-bound homochiral and heterochiral complexes than mentioned above

The collision-energy dependent study of the dissociation of $[(1H)I(2H)]^+$ does indeed reveal that the elimination of HI is important only at low collision energies (Fig. 3). It is consistent with the fact that the primarily iodide-bound complex of two protonated bases has to rearrange to a proton-bound complex of the two bases and HI molecule and, therefore, it cannot compete at large collision energies with direct fragmentations. Figure 3 shows the ion yields corresponding to the elimination of HI (in red) and to a simple cleavage of the iodide-bound complex (in blue) in dependence on the collision energy. The breakdown pattern of the heterochiral complex generated from *S*-**1** and *R*-**2** looks very similar and no chiral effect is obvious from the data. Note that the experiment is conducted at single-collision conditions, which means that a substantial part of the studied ions does not undergo any collision and therefore does not fragment even at large collision energies (i.e. here, 40% of parent ions remain intact even at collision energies exceeding 5 eV).

A chiral effect can be found if only the ratio between the abundance of the HI elimination (fragment $[(1)H(2)]^+$ with m/z 214) and the formation of $1H^+$ (m/z 141) is considered (thus the two channels indicated in Scheme 4). Figure 4 shows the dependence of this ratio on the collision energy for the homochiral complex $[(S-1\cdot H)I(S-2\cdot H)]^+$ (black line) and the heterochiral complex $[(S-1\cdot H)I(R-2\cdot H)]^+$ (blue line). An average chiral effect²⁹ is evaluated

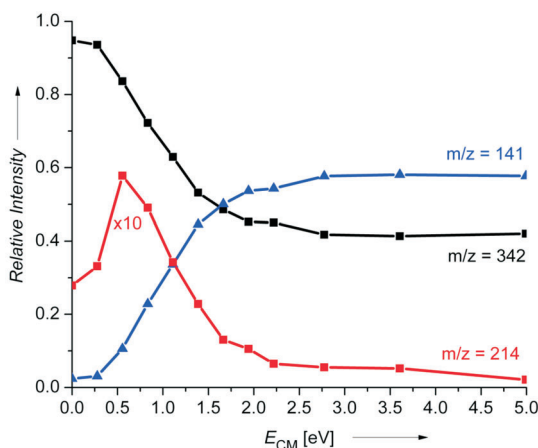


FIG. 3

Fragmentation of the $[(S-1\cdot H)I(S-2\cdot H)]^+$ complex in dependence on the collision energy. The ion yield denoted by $m/z = 141$ (blue curve) corresponds to the sum of the abundances of the ions with m/z 141, 124, 74, and 57

as an average ratio according to the Eq. (1) in the range of collision energies 0–1.1 eV and it amounts to 1.2.

$$\frac{K_{\text{homo}}}{K_{\text{hetero}}} = \frac{[(S-1)H(S-2)]^+ / [(S-1)H]^+}{[(S-1)H(R-2)]^+ / [(S-1)H]^+} \quad (1)$$

The values obtained at higher collision energies are not considered, because firstly the abundance of the fragment $[(1)H(2)]^+$ is close to zero and therefore these values bear large experimental errors and, secondly, due to the energy dependence of the chiral effect, these values are close to unity. Seemingly, the enantioselectivity of the reaction peaks at 0.3 eV. According to the theory, the chiral effect should be continuously decreasing with the increasing collision energy. The drop in the intensity at the zero collision energy can be regarded as an experimental artifact due to the very low intensities of the ion currents at this special experimental arrangement.

The experimental results obtained nicely complement the results of the DFT calculations. Thus, the elimination of the HI molecule can only compete at low collision energies. For the homochiral $[(1H)I(2H)]^+$ complex, the elimination of HI is slightly less endothermic than the cleavage of the com-

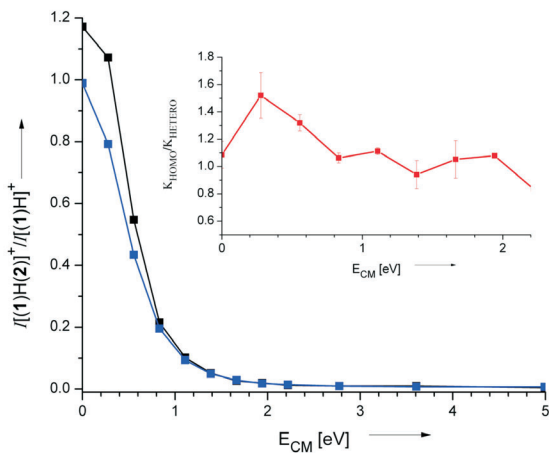


FIG. 4

Ratio of the abundances of $[(1)H(2)]^+$ (m/z 214) and $1H^+$ (m/z 141) generated by CID of the parent ion $[(S-1)H]I[(S-2)H]^+$ (black line) and $[(S-1)H]I[(R-2)H]^+$ (blue line), respectively, in dependence of the collision energy. The inset shows the chiral effect as defined by Eq. (1) obtained as an average of two independent measurements. The error bars show the standard error of the mean

plex into $1\cdot\text{H}^+$ and $2\cdot\text{HI}$. Accordingly, at collision energies close to zero the elimination of HI prevails over the complex cleavage. On the other hand, for the heterochiral $[(1\text{H})\text{I}(2\text{H})]^+$ complex, the HI elimination requires more energy than complex cleavage and, accordingly, the HI elimination never exceeds the complex cleavage in the experiment. The delicate differences on the potential-energy surface also result in energy dependence of the chiral effect as demonstrated in the inset in Fig. 4. Thus, the largest effect can be found at energies close to zero. The experimentally found chiral effect is smaller than it would be expected based on calculations, which is most probably due to the inherent shortcomings of the experiment. The kinetic energy resolution of the parent ions in the center-of-mass frame is ca. 50 kJ/mol (full width at half-maximum) and therefore, the measured chiral effect is distorted by higher-energy contributions.

It can be expected that the differences between homochiral and heterochiral diastereoisomeric complexes of **1** become much more pronounced, if the metal-bound complexes instead of proton-bound complexes are considered. The metal ions will most probably bind to both nitrogen atoms of **1** and therefore the whole cavity of the base will participate in the steric interactions with the other partners in the complex. These complexes will be subject of future studies.

CONCLUSIONS

Experimental and theoretical studies of the proton-bound complexes of 1,5-diaza-*cis*-decalin (**1**) and butan-2-amine (**2**) ($[(1)\text{H}(2)]^+$) and the iodide-bound complexes $[(1\text{H})\text{I}(2\text{H})]^+$ reveal that the homochiral combination of the two bases is preferred. DFT calculations show that the elimination of HI from homochiral $[(1\text{H})\text{I}(2\text{H})]^+$ is slightly less endothermic than the complex cleavage to yield $1\cdot\text{H}^+$ and $2\cdot\text{HI}$, whereas for the heterochiral variant the complex cleavage is less endothermic. In accordance, CID of homochiral $[(1\text{H})\text{I}(2\text{H})]^+$ at the collision energies close to zero leads to a larger abundance of $[(1)\text{H}(2)]^+$ compared to $1\cdot\text{H}^+$. On the other hand, formation of $1\cdot\text{H}^+$ always exceeds that of $[(1)\text{H}(2)]^+$ in the CID of heterochiral $[(1\text{H})\text{I}(2\text{H})]^+$. Due to these differences on the potential-energy surface, the chiral effect is slightly dependent on the collision-energy and an average value of 1.2 is determined as an average for collision energies in the range of 0–1.1 eV.

This work was supported by the Academy of Sciences of the Czech Republic (Z40550506) and the Ministry of Education, Youth and Sports of the Czech Republic (MSM0021620857).

REFERENCES

1. Kozłowski M. C., Li X., Carroll P. J., Xu Z.: *Organometallics* **2002**, *21*, 4513.
2. Santos A. G., Klute W., Torode J., Bohm V. P. W., Cabrite E., Runsink J., Hoffmann R. W.: *New J. Chem.* **1998**, *22*, 993.
3. Singh A., Chakraborty S., Ganguly B.: *Eur. J. Org. Chem.* **2006**, 4938.
4. Roithová J., Schröder D.: *Phys. Chem. Chem. Phys.* **2007**, *9*, 713.
5. Roithová J., Schröder D., Míšek J., Stará I. G., Starý I.: *J. Mass Spectrom.* **2007**, *42*, 1233.
6. Vosko S. H., Wilk L., Nusair M.: *Can. J. Phys.* **1980**, *58*, 1200.
7. Lee C., Yang W., Parr R. G.: *Phys. Rev. B* **1988**, *37*, 785.
8. Miehlich B., Savin A., Stoll H., Preuss H.: *Chem. Phys. Lett.* **1989**, *157*, 200.
9. *Gaussian 03*, Revision C.02. Gaussian, Inc., Wallingford, CT 2004.
10. Dunning T. H., Jr., Hay P. J. in: *Modern Theoretical Chemistry* (H. F. Schaefer III, Ed.), Vol. 3, pp. 1–28. Plenum Press, New York 1976.
11. Fuentealba P., Preuss H., Stoll H., v. Szentpaly L.: *Chem. Phys. Lett.* **1989**, *89*, 418.
12. Le Barbu K., Brenner V., Millie P., Lahmani F., Zehnacker-Rentien A.: *J. Phys. Chem. A* **1998**, *102*, 128.
13. *NIST Standard Reference Database Number 69*, Gaithersburg, 2005, see: <http://webbook.nist.gov/chemistry/>.
14. Sawada M.: *Mass Spectrom. Rev.* **1997**, *16*, 733.
15. Schalley C. A.: *Int. J. Mass Spectrom.* **2000**, *194*, 11.
16. Lebrilla C. B.: *Acc. Chem. Res.* **2001**, *34*, 653.
17. Filippi A., Giardini A., Piccirillo S., Speranza M.: *Int. J. Mass Spectrom.* **2000**, *198*, 137.
18. Dearden D., Liang Y., Nicoll J. B., Kellersberger K. A.: *J. Mass Spectrom.* **2001**, *36*, 989.
19. Le Barbu K., Zehnacker A., Lahmani F., Mons M., Piuze F., Dimicoli I.: *Chirality* **2001**, *13*, 615.
20. Schröder D., Schwarz H.: *Top. Curr. Chem.* **2003**, *225*, 133.
21. Speranza M.: *Int. J. Mass Spectrom.* **2004**, *232*, 277.
22. Tureček F.: *Mass Spectrom. Rev.* **2007**, *26*, 563.
23. Fales F. H., Wright G. J.: *J. Am. Chem. Soc.* **1977**, *99*, 2339.
24. Cooks R. G., Kruger T. L.: *J. Am. Chem. Soc.* **1977**, *99*, 1279.
25. Cooks R. G., Patrick J. S., Kotiaho T., McLuckey S. A.: *Mass Spectrom. Rev.* **1994**, *13*, 287.
26. Ramirez J., Ahn S., Grigorean G., Lebrilla C. B.: *J. Am. Chem. Soc.* **2000**, *122*, 6884.
27. Tafi A., Botta B., Botta M., Delle Monache G., Filippi A., Speranza M.: *Chem. Eur. J.* **2004**, *10*, 4126.
28. Gatlin C. L., Tureček F., Vaisar T.: *Anal. Chem.* **1994**, *66*, 3950.
29. Schröder D., Schwarz H.: *Int. J. Mass Spectrom.* **2004**, *231*, 139.